Magnetic configuration effects on the radial electric field and the Reynolds stress in the plasma edge

P. Manz[1], G. Birkenmeier[2,1], M. Cavedon[1], N. Fedorczak[3], S. Garland[4], U. Plank[1], M. Ramisch[4], T. T. Ribeiro[1], B. Schmid[4], B. D. Scott[1]

[1] *Max-Planck-Institut für Plasmaphysik, 85748 Garching, Germany*

[2] *Physik-Department E28, Technische Universität München, 85748 Garching, Germany*

[3] *CEA, IRFM, F-13108 Saint-Paul-Lez-Durance, France*

[4] *Institut für Grenzflächenverfahrenstechnik und Plasmatechnologie, Universität Stuttgart, 70569 Stuttgart, Germany*

The poloidal position of the X-point or the end plates in the scrape-off layer are known to influence the radial electric field and, therefore, the confinement in the edge of a magnetically confined plasma. The interaction of the radial electric field with the turbulence is described by the Reynolds stress, which is determined by the tilt of the turbulent structures as well as their amplitude. In the scenario presented in Ref. [1] the $\hat{s}$-residual Reynolds stress induced by the magnetic shear may act as a seed tilt which can be self-amplified by the interaction of zonal flows and turbulence leading to differences in the radial electric field for magnetic configurations. The $\hat{s}$-residual Reynolds stress is given by $\Pi_{\hat{s}} = -\hat{s}\theta\langle\tilde{u}_x^2\rangle$ [1, 2], where $\hat{s}$ is the magnetic shear, θ the poloidal ballooning angle and $\tilde{u}_x$ the radial $E \times B$ velocity of the fluctuations. The basic idea is that structures born at the outboard midplane and following the magnetic field lines are tilted by the magnetic shear. The tilt of the structures is equivalent to the Reynolds stress. In the case of a poloidally symmetric plasma, $\langle\Pi_{\hat{s}}\rangle$ vanishes. An imbalance between positive tilt and negative tilt can be provided by a poloidal truncation of the ballooning envelope. This can be justified by X-point resistivity for diverted plasmas or by end-plates boundaries for limited plasmas, which could induce a feedback to the confined region [1, 2].

Simulations have been carried out with the three-dimensional gyrofluid electromagnetic turbulence model GEMR [3, 4]. A circular plasma cross-section with toroidal axisymmetry is implemented. The coordinate system is aligned with the equilibrium magnetic field. The radial coordinate is x, the parallel coordinate is s and the binormal coordinate is y. Although being a δ-f limited code the gradients evolve freely, as required by the strength of fluctuating dynamics in this plasma region. Since the profiles are included in the dependent variables and in the polarization, GEMR is a global model. Also the background radial electric field evolves self-consistently. However, the deviation from the preset background values has to be small.

To gain confidence in the simulations a small laboratory plasma is simulated first, where

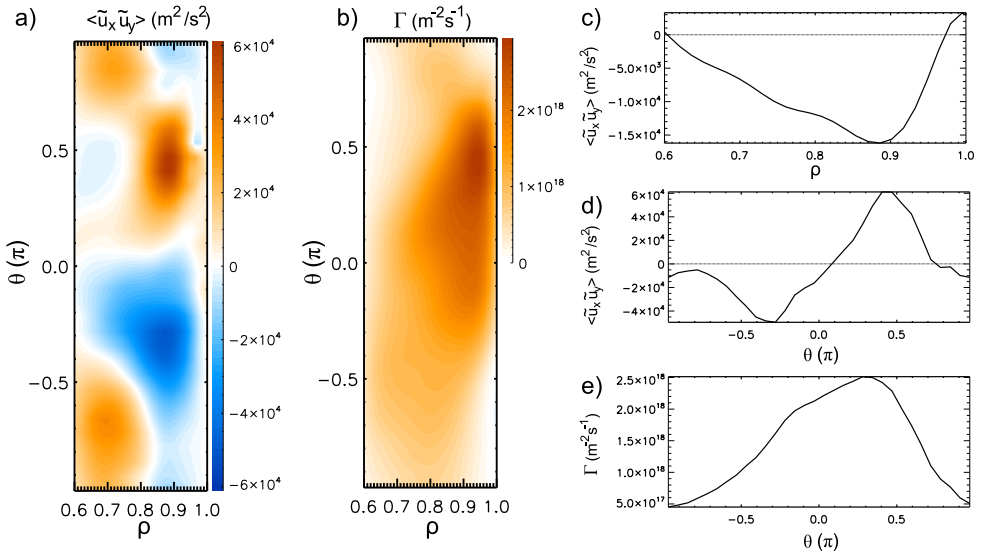

Figure 1: *Poloidally and radially resolved Reynolds stress (a) and transport (b). Reynolds stress profile at the outboard midplane (c), Poloidally resolved Reynolds stress (d) and transport (e) at the position of strongest Reynolds stress at* $\rho = 0.88$*. Data are from GEMR simulation.*

the poloidal distribution of the Reynolds stress is known. Poloidally resolved measurements of the Reynolds stress in a magnetically confined plasma are only available from the stellarator TJ-K [5]. The stellerator TJ-K ($R = 0.6$ m, $a = 0.12$ m) is usually operated at a low magnetic field of $B = 72$ mT. The experiments have been performed in helium ($A = 4$) at a density of $n_e = 1.5 \cdot 10^{17}$ m^{-3} and an electron temperature of $T_e = 10$ eV. The ions are cold. It seems a bit audacious to simulate a stellerator with a circular tokamak plasma, but the probe array is located at the very edge of the plasma at an outer port, where the local magnetic field is in first order similar to a tokamak, as it can be seen from the sinusoidal variation of the curvatures (Fig. 2c in Ref. [5]). At the probe array position the corresponding safety factor is $q_s = 4.5$ with low magnetic shear $\hat{s} = -0.16$. Turbulence in TJ-K is driven by the density gradient, the electron temperature is rather flat. This translates to the following GEMR input parameters: $\delta = 0.10$, $\beta = 5.83 \cdot 10^{-5}$, $\nu = 1.25$ and $\tau_i = 0.1$. The initial density gradient scale has been chosen to be $L_n = 3$ cm, electron and ion gradient scales vanish, i.e. $L_{Te} = L_{T_i} = 0$. The simulation has been done on a $32 \times 64 \times 32$ grid.

The poloidally resolved Reynolds stress $\langle \tilde{u}_x \tilde{u}_y \rangle_{y,t}$ is shown in Fig. 1a. The poloidal angle is defined as in Ref. [5], starting at the outboard midplane $\theta = 0$ and moving counterclockwise to the top, high field side and bottom. The Reynolds stress is also defined as in Ref. [5], which means that an outward velocity $\tilde{u}_x > 0$ and the binormal velocity in the ion diamagnetic direction, $\tilde{u}_y > 0$, lead to a positive Reynolds stress. In amplitude the Reynolds stress is much

smaller in this simulation compared to the experiment. This might be a consequence of the δ-f approach. The spatial distribution of the Reynolds stress obtained with the simulation is quite similar to the experiment. On the outboard midplane, $\theta = 0$, the Reynolds stress is negative and exhibits its minimum at $\rho \approx 0.9$ (Fig.1c) similar to the experiment (see Fig. 2a in Ref. [5]). Furthermore, the Reynolds stress shows a strong poloidal asymmetry. At $\rho = 0.88$, which roughly corresponds to the probe array position, the maximum of the Reynolds stress is located at $\theta \approx 0.4\pi$ (Fig.1d) as in the experiment (Fig. 2b in Ref. [5]). However, the overall asymmetry is stronger pronounced in the GEMR simulation. Also the transport shows a strong poloidal asymmetry. This has been also reported for TJ-K [6]. The maximum of the Reynolds stress is at a similar position as the maximum of the transport in the TJ-K experiments [5, 6], which is recovered by the present simulation (see Figs. 1a and b or Figs. 1d and e).

In a second step, the impact of the poloidal limiter position on the radial electric field and the Reynolds stress is studied at ASDEX Upgrade parameters. The limiter positions mimic the lower single null ($\theta_X = -0.5\pi$) and the upper single null ($\theta_X = +0.5\pi$) configuration. For ASDEX Upgrade ($R = 1.65$ m, $a = 0.5$ m, $B = 2.5$ T) typical experimental parameters at the last closed flux surface (LCFS) as the reference flux surface are chosen to be $n_e = 1 \cdot 10^{19}$ m^{-3}, $T_e = T_i = 100$ eV, $q_s = 4.6$, $\hat{s} = 1.35$ and initial gradient scale lengths of $0.5L_n = L_{Te} = L_{Ti} = 2.5$ cm. These translate to the following GEMR input parameters: $\delta = 1.2 \cdot 10^{-3}$, $\beta = 3 \cdot 10^{-5}$ and $\nu = 2.94$. The simulations have been done on a $128 \times 512 \times 16$ grid.

The results are shown in Fig. 2. The radial electric field E_r roughly follows $(\nabla p_i)/en$ in the confined region and $-(3/e)\nabla T_e$ in the SOL (Figs. 2a,b), as it is the typical case for ASDEX Upgrade plasmas. As $\nabla p_i/en$ has been set to be similar for both configurations also E_r is similar. The difference between E_r and $\nabla p_i/en$ maybe attributed to the zonal flow and is small, in agreement to recent ASDEX results [7]. The deviation of $\nabla p_i/en$ from E_r is larger in the lower limiter case, at the very edge, close to the LCFS (Figs. 2a and b). Since the ion diamagnetic velocity is defined negative for easier comparison with [1, 2], the shear is negative. The zonally averaged Reynolds stress $\langle \tilde{u}_x \tilde{u}_y \rangle_{y,s,t}$ is nearly a factor of two larger close to the LCFS (Figs. 2c,d). In the SOL the zonally averaged Reynolds stress changes sign. This can be attributed to the $\hat{s}$-residual stress. As seen in (Figs. 2e,f) the Reynolds stress $\langle \tilde{u}_x \tilde{u}_y \rangle_{y,t}$ follows the tilt of the magnetic shear along the field lines. At the limiter the ballooning envelope is truncated. This leads to an imbalance between positive tilt and negative tilt, which can be amplified. Due to this amplification the Reynolds stress is much higher than the seed stress provided by $\Pi_{\hat{s}}$. At the LCFS (Figs. 2g,h) the Reynolds stress follows the magnetic tilt at the outboard side, at the inboard side a qualitative discrepancy is observed as the structures are tilted back.

In the confined region (Figs. 2i,j) the Reynolds stress has a sinusoidal shape in the poloidal plane as in the TJ-K case (Figs. 1a,d). As the LCFS connects the confined region with the SOL it exhibits features of both regions. Nevertheless, the truncation and the accompanying residual stress is clearly observable at the LCFS.

As the simulations also show, the Reynolds stress is varying strongly on the poloidal plane, therefore measurements at one poloidal positions are not representative. To draw conclusions from such measurements a detailed understanding of the poloidal asymmetry of the Reynolds stress is needed.

Please note, all results presented in this contribution are preliminary and may be subject to change.

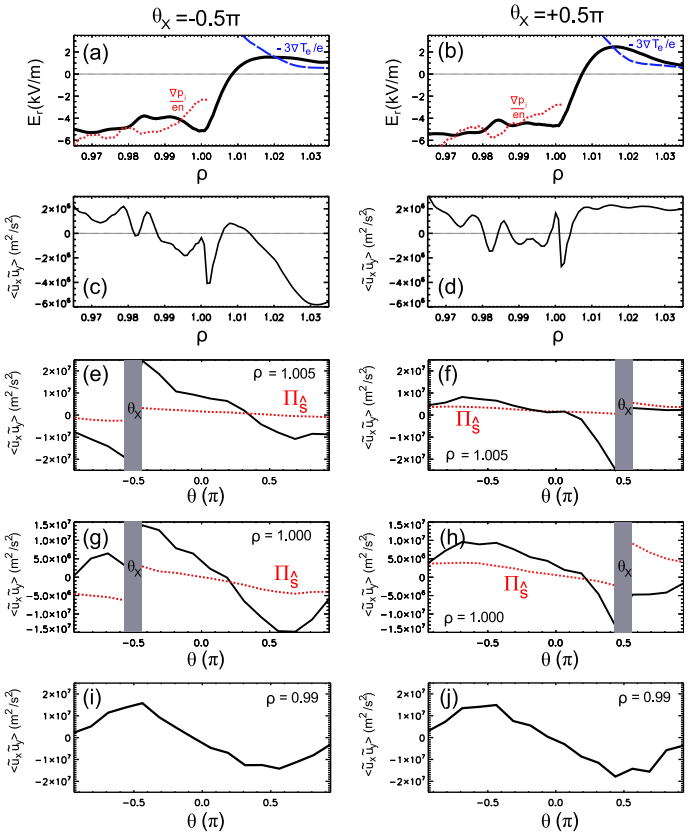

Figure 2: *Radial electric field (a,b), zonal averaged Reynolds stress (c,d), Reynolds stress and $\Pi_{\hat{s}}$ in the near SOL ($\rho = 1.005$) (e,f), at the LCFS ($\rho = 1.000$) (g,h) and inside the very edge of the confined region ($\rho = 0.99$). The lower limiter case ($\theta_X = -0.5\pi$) is shown on the left hand side, the upper limiter case ($\theta_X = +0.5\pi$) on the right hand side.*

This work has been carried out within the framework of the EUROfusion Consortium and has received funding from the Euratom research and training programme 2014-2018 under grant agreement No 633053. The views and opinions expressed herein do not necessarily reflect those of the European Commission.

References

[1] N. Fedorczak et al., Nuclear Fusion **52**, 103013 (2012)

[2] N. Fedorczak et al., Plasma Phys. Control. Fusion **55**, 124024 (2012)

[3] B.D. Scott, Contr. Plasma Phys. **46**, 714 (2006)

[4] A. Kendl et al., Phys. Plasmas **17**, 072302 (2010)

[5] B. Schmid et al., New. J. Phys. **19**, 055003 (2017)

[6] G. Birkenmeier et al., Phys. Rev. Lett **107**, 025001 (2011)

[7] M. Cavedon et al., Nuclear Fusion **72**, 014002 (2017)